AIAA Propulsion and Energy Forum
August 9-11, 2021, VIRTUAL EVENT
AIAA Propulsion and Energy 2021 Forum

10.2514/6.2021-3399

Check for updates

Anomalous electron thermal conductivity in a magnetic nozzle

Shadrach Hepner*
University of Michigan, Ann Arbor, MI, 48109

Benjamin A. Jorns†
University of Michigan, Ann Arbor, MI, 48109

The impact of plasma instabilities on the electron thermodynamics of a magnetic nozzle is investigated. An expression is derived for an effective collision frequency between electrons and ions that results from a wave-induced resistive force in the parallel direction to the nozzle's magnetic field. This collision frequency is then incorporated into the classical heat conduction term in the electron energy equation to find an expression for an effective polytropic index. An experiment is performed on an electron cyclotron resonance thruster at 17 W to evaluate this expression. Measurements are performed of both the background plasma properties and wave propagation characteristics. Experimental measurements indicate a polytropic index of 1.15 $\pm .1$. This result is compared to the instability-driven theory which predicts a polytropic index that varies between 1 and 1.1, comparing well with measurements. The results are discussed in the context of thruster energy balance, and several potential error sources are addressed.

Downloaded by UNIV OF MICHIGAN on August 31, 2021 | http://arc.aiaa.org | DOI: 10.2514/6.2021-3399

Nomenclature

n	=	Number density
A	=	Effective magnetic nozzle area
u	=	Bulk velocity
T	=	Temperature
q	=	Heat flux
ϕ	=	Plasma potential
m	=	Particle mass
γ	=	Polytropic index
f	=	Distribution function
α	=	Initial condition $T_0/n_0^{\gamma-1}$
q	=	Species charge
E	=	Electric field
B	=	Magnetic field
R_{an}	=	Anomalous resistivity
P	=	Pressure
ν	=	Collision frequency
χ	=	Susceptibility
ω	=	Frequency
k	=	Wavenumber
ϵ_0	=	Permittivity of free space
Z	=	Particle charge state
$F_{M,e}$	=	Maxwellian electron distribution function
v_θ	=	azimuthal velocity
v_E	=	Electron $E \times B$ drift
V_D	=	Electron diamagnetic drift
$\omega_{p,i}$	=	Ion plasma frequency
v_ϕ	=	Phase velocity

*PhD Candidate, Department of Aerospace Engineering, AIAA Student Member
†Assistant Professor, Department of Aerospace Engineering, AIAA Associate Fellow

Copyright © 2021 by the American Institute of Aeronautics and Astronautics, Inc. All rights reserved.

Downloaded by UNIV OF MICHIGAN on August 31, 2021 | http://arc.aiaa.org | DOI: 10.2514/6.2021-3399

I. Introduction

MAGNETIC nozzles are a type of electric propulsion that generate thrust by expanding a heated plasma through a diverging magnetic field. The plasma propellant typically is heated by an electrodeless radiofreqency or microwave antenna in a discharge chamber. The energized propellant then diffuses out of the chamber and is further accelerated by diamagnetic currents interacting with the applied magnetic field. These devices are believed to exhibit long lifetimes and to be propellant ambivalent, which is ideal for long-duration missions that may require mid-flight refueling.

Low power, smaller nozzles (i.e. under or around 100 W) are typically considered "electron-driven," meaning that the heating is applied directly to the electrons. This is the case because many wave heating schemes (i.e. helicon or electron cyclotron resonance) require particles to be magnetized, and magnetized ions require prohibitively high magnetic fields at the small lenghtscale of 100 W class devices. The high temperature electrons then accelerate out of the nozzle aided by the interaction with the applied field. As they do so, the cold ions are dragged by an ambipolar electric field from the electrons that accelerate them downstream. Thus, the nozzle converts electron thermal energy into bulk ion energy, which translates directly to thrust.

While this principle of operation is relatively well understood, a complete description of the details of the evolution of electron energy remains elusive. Typically in order to model such a plasma, one of several assumptions about the thermal decay is applied. The first such assumption is that of isothermal electrons. It is often argued that the electron temperature is constant along field lines because the electrons are highly mobile on this axis, and any temperature gradients would instantly be relaxed. However, while this approximation may be valid for estimating upstream temperatures from a downstream measurement, it breaks down when used to model the thermal expansion physically. Indeed, it has been shown [1] that the isothermal situation implies an infinite heat flux from the nozzle itself, which violates energy conservation. Alternatively, electron adiabaticity has also been theorized. This assumption is convenient for its straightforward analogue to conventional, neutral gas nozzles and neglects heat flux and collisional heating. However, this case classically requires a high collision rate, which is not often the case in these plasmas.

Measurements to date have shown that neither of these extremes in heat conduction—isothermal or adiabatic— is correct. A multitude of measurements have shown that electrons cool as they expand and thus are not isothermal. At the same time, the degree of cooling is too weak to be considered adiabatic [2, 3], except under rare conditions [4]. It is thus evident that either heating or heat flux must be significant in a magnetic nozzle expansion. With this in mind, there have been several recent attempts to reconcile theory with experiment on this issue. Zhang et al. [5] theorized that the observed trends in temperature may be predicted by a non-local, non-equilibrium treatment of the electrons. They derived a thermodynamic model of an expanding electron fluid with a depleted high energy population that accurately predicts electron temperature decay with expansion. However, this theory is predicated on a collisionless environment, which has been shown to not be satisfied for some lower power nozzles [2]. As an alternative explanation, Ahedo et al. [6] showed through a quasi one dimensional fluid-based model that if it is assumed that there is an equivalence between conducted and convected heat flux, it is possible to create temperature profiles consistent with experiment. However, this approach was limited in that it was largely phenomenological and not based on a first-principles argument. Finally, Little and Choueri [2] argued that adoption of a classical heat conduction, i.e. a Fourier-like law governed by collisions, can explain measured trends in electron cooling in their experiment. However, they noted that in practice, the magnitude of the classical collision frequency was too low, which led to a nonphysical heat flux downstream greater than the power delivered to the thruster. The authors thus concluded that even if the scaling of a Fourier law is appropriate, a higher collision frequency would be required to physically explain the expansion.

While all of these theories are applicable in certain situations, the final one is particularly intriguing in light of recent experimental work that has shown that plasma instabilities may be a source for enhanced, non-classical collisionality [7] in the nozzle plume. Indeed, plasma instabilities have been shown to lead to enhanced, "anomalous" resistivity in a variety of plasmas [8–14], and we recently have observed a lower hybrid drift instability in a magnetic nozzle plume that induces an effective collision frequency several orders of magnitude higher than the classical equivalent [7]. It stands to reason that the problem illustrated in Ref. [2] of heat flux higher than thruster power may be resolved then with the inclusion of anomalous effects, and a modified Fourier law may be usable in these situations. Thus, given the role of instabilities in inducing an anomalous collision frequency higher than the classical value and the inconsistency of classical collisions in magnetic nozzle expansion, the need is apparent to analyze the applicability of an anomalous collision frequency in impeding heat flux.

This work presents a first analysis of the applicability of anomalous effects to a Fourier law of heat transport in a magnetic nozzle. To this end, we organize this paper in the following way. We outline the theory behind anomalous heat transport and the theorized polytropic index in Sct. II. We then proceed to outline the experiment that we performed in

Downloaded by UNIV OF MICHIGAN on August 31, 2021 | http://arc.aiaa.org | DOI: 10.2514/6.2021-3399

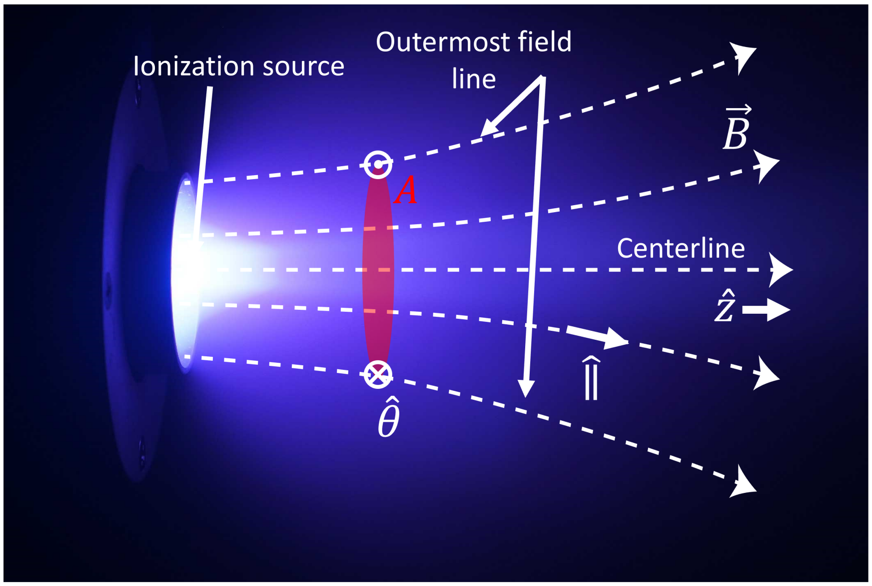

Fig. 1 Illustration of a paraxial model.

Sct. III and outline the results as applicable to the current analysis in Sct. IV. Finally, we discuss the results and the correlation between theory and experiment in Sct. V and provide concluding remarks in Sct. VI.

II. Theory

In this section we establish the mathematical formalism that forms the basis of the current hypothesis. We first introduce a quasi one dimensional geometry that we will apply for this work. We then motivate the study of thermal energy patterns based on thruster performance. Next, we introduce the polytropic assumption as a closure scheme for the fluid equations. We then progress into a discussion of the electron energy equation and various closure schemes for it, introducing the Fourier law and discussing how it relates to the polytropic index. Finally, we outline the impact that waves may have on enhancing this collision frequency and relate it to our prediction of heat flux and the polytropic index.

A. Geometry and coordinate convention

We begin by describing the geometric framework that will inform the theory that we use for this study. We will assume a quasi one-dimensional flow [2, 6, 15], where all quantities vary only in the axial direction and we incorporate a varying area $A(z)$. We define this area as the circular cross section with its outer edge coinciding with the outermost field line that intersects the thruster exit plane (Fig. 1). We define z as the direction along centerline and $\|$ as the local direction along the magnetic field, with θ being the azimuthal direction.

We now apply this paradigm to the steady-state fluid equations. We start with continuity, which we acquire by volumetrically integrating over cross-sectional area A. Doing so shows

$$(n_s u_s A)' = 0 \tag{1}$$

where n is the number density, u is the velocity, and a subscript s indicates an arbitrary species and the prime indicates d/dz. We also may find an equivalent energy equation, starting with a generalized form assuming that pressure $P = nT$ with T being the temperature, and further assuming zero resistivity:

$$0 = \frac{3}{2}\mathbf{u} \cdot \nabla(n_s T_s) + \frac{5}{2} AnT\nabla \cdot \mathbf{u} + \nabla \cdot \mathbf{q} \tag{2}$$

$$= \frac{3}{2}u(n_s T_s)' + \frac{5}{2}nT(uA)' + (qA)', \tag{3}$$

Where q is the heat flux. The first two terms of this equation represents the total fluid energy change from acceleration and convection, and the final term represents the heat flux term, i.e. conduction. Here, we have again neglected Ohmic

Downloaded by UNIV OF MICHIGAN on August 31, 2021 | http://arc.aiaa.org | DOI: 10.2514/6.2021-3399

heating and collisional heat transfer, which would contribute further terms. Now that we have established the paraxial model that we are going to use in this analysis, we will explain the significance of the thermal energy decay with this paradigm.

B. Relationship between specific impulse and temperature

Magnetic nozzles are thermally driven. As the main mechanism for thrust production is the conversion of thermal electron energy into ion kinetic energy, the electron thermodynamics plays a crucial role. This energy conversion relies on a plasma potential drop as an intermediate. To explore this concept, we reference the coordinate convention shown in Fig. 1 and consider the simplified case of a collisionless electron Ohm's law in the direction parallel to the applied magnetic field:

$$0 - (n_e T_e)' + \frac{ne}{m_e}\phi' \tag{4}$$

$$\phi' = \frac{m_e}{e}\frac{(n_e T_e)'}{n_e} \tag{5}$$

where ϕ os the plasma potential, e is the electron charge, m_e as the electron mass, and ϕ as the plasma potential. The relatively massless electrons thus induce an electric field along field lines through this expansion.

The ions carry the majority of the momentum in the plasma, and thus may be taken as a reliable proxy for thrust production. Even though the thrust is directly produced by the electron pressure and the diamagnetic currents interacting with the magnets, conservation of momentum dictates that the total momentum flux leaving the system is equivalent to the thrust production. As such, accelerating the ions is equivalent to producing thrust. As they are not directly heated, they are unlikely to maintain a significant pressure. However, the inertial term in the ion momentum equation is important given their higher mass. In steady state,

$$\frac{m_i}{2}(u_i^2)' = e\phi' \tag{6}$$

$$= \frac{(n_e T_e)'}{n_e}. \tag{7}$$

This simple analysis reveals that a decreasing electron thermal energy is converted directly into bulk ion kinetic energy. However, this does not provide a complete description of the plasma. Indeed, while we might motivate expressions for how the density will decrease due to expansion of the plume, we do not know a priori how the temperature will vary. A closure model for electron energy, i.e. an equation that relates the temperature to other more easily inferred parameters like plasma density, is still required.

C. Polytropic law for electron energy

A common method for inferring the varying electron temperature in nozzles is to assume an equation of state based on a polytropic law:

$$\frac{T_e}{n^{\gamma-1}} = \alpha \tag{8}$$

where α is a constant along an electron streamline and γ is the so-called polytropic index. Setting the derivative of this form equal to zero and integrating along a streamline provides a means of directly measuring the value of γ locally:

$$\gamma = 1 + \frac{\ln(T/T_0)}{\ln(n/n_0)} \tag{9}$$

where the subscripts 0 indicate an upstream position. Closing the fluid equations in such a way provides a convenient way to solve them; however, predicting the value of γ proves to be more of a challenge.

Previously, a computational study has been performed that allowed γ to vary as a free parameter in a magnetic nozzle expansion [1]. This work found that a lower γ implied a higher heat flux downstream, which in turn ultimately was converted to ion energy and enhanced specific impulse. This correlation between γ and specific impulse motivates the current study on what may cause γ to take a given value.

Downloaded by UNIV OF MICHIGAN on August 31, 2021 | http://arc.aiaa.org | DOI: 10.2514/6.2021-3399

D. Estimating polytropic index based on closure models for electron flux

While the energy equation subject to the paraxial approximation allows us an extra equation to solve for T_e, we have introduced an even higher moment of the distribution function in allowing the heat flux to be finite, and must find a way of closing the fluid equations by making an assumption regarding the heat flux. Commonly, this value can be taken to be either zero (adiabatic limit) or infinity (isothermal limit), and looking at these limits provides a means of physically bounding γ.

1. Adiabatic approximation

In an expanding nozzle, heat flux is often assumed to be zero, resulting in the adiabatic limit. This approximation is successfully used for conventional nozzles and provides a convenient closure for the plasma case as well. This assumption further makes physical sense, since a fully Maxwellian distribution function has zero heat flux. To understand why, we may look at the kinetic definition:

$$\mathbf{q} = \frac{m}{2}\int (\mathbf{v}-\mathbf{u})^3 f(\mathbf{v})d\mathbf{v} \tag{10}$$

with $f(\mathbf{v})$ being the distribution function. This is an odd moment taken over the random (i.e. zero-mean) velocity, meaning that any distribution function that is symmetric about its mean velocity will give zero heat flux. A drifting Maxwellian distribution fulfills this criterion and thus does not conduct heat. The energy equation that results is [16]

$$0 = uA(nT)' + \frac{5}{3}nT(uA)' \tag{11}$$

$$= \frac{T'}{T} - \frac{2}{3}\frac{n'}{n} \tag{12}$$

where we have used the continuity equation to substitute $n(uA)' = -n'uA$. Performing the integration, we see that

$$\frac{T}{n^{2/3}} = \text{const.} \tag{13}$$

Thus, the adiabatic assumption yields $\gamma = 5/3$.

2. Isothermal approximation

Taking the limit in the opposite direction $\mathbf{q} \to \infty$ gives the other physical bound of γ. In this case, the heat flux overcomes any temperature gradients immediately, implying that T_e =const. Applying this to the polytropic law, we see that $\gamma = 1$. Thus, γ varies with the magnitude of the heat flux and should be bound by 1 or $5/3$. However, this index has been measured previously and is generally found to take an intermediate value between these two limits [2–4]. To explore this possibility, a more precise form for $\mathbf{q}$ is needed.

3. Fourier law for heat conduction

Finite heat flux is a potential route to changing the value of γ between the isothermal and adiabatic limits. Often, a Fourier law is assumed, where heat travels down a temperature gradient and is impeded by collisions [17]. This law takes the form

$$\mathbf{q} = -3.2\frac{nT\nabla T}{m\nu}, \tag{14}$$

where ν is the electron collision frequency. This law provides a closure to the fluid equations, since the higher moment value ($\mathbf{q}$) is replaced by values of lower moments of the distribution function. Substituting this form for $\mathbf{q}$ and further assuming a polytropic law for T_e allows us to find a value for γ.

4. Form for γ

We may now use the Fourier law and the polytropic assumption in the energy equation to find a relation for γ. We relpace the temperature with the polytropic form, finding

$$T_e = \alpha n^{\gamma-1} \tag{15}$$

$$T_e' = \alpha(\gamma-1)n^{\gamma-2}n' \tag{16}$$

where we have defined $\alpha = T_{e,0}/n_0^{\gamma-1}$. Inserting these definitions and the Fourier law (Eqn. 14) into the energy equation yields

$$\left(\gamma - \frac{5}{3}\right)\frac{2}{3}un' - (\gamma - 1)\,\frac{3.2\alpha n^{\gamma-1}n'}{m_e\nu}\left[\frac{A'}{A} + \frac{2(\gamma-1)n'}{n} + \frac{n''}{n'} - \frac{\nu'}{\nu}\right] = 0. \tag{17}$$

The first term on the left represents convection and the second term represents conduction and expansion effects. If collisions are frequent, the heat conduction becomes negligible (adiabatic), and $\gamma = 5/3$. When collisions are infrequent, the right side dominates and two possible solutions appear. The first is simply $\gamma = 1$, which is typically the isothermal limit. However, in the current experiment, this solution always takes a true value slightly under 1, which is nonphysical. Thus we may discard this solution.

However, a second solution is present as well. Namely, the term in square brackets can be set equal to zero and solved for γ as

$$\gamma = 1 - \frac{nA'}{2n'A} + \frac{n''n}{2(n')^2} - \frac{\nu' n}{2\nu n'}. \tag{18}$$

This equation provides the value for γ in the low collision frequency limit. In the zero-expansion limit ($A' = n' = \nu' = 0$), we recover the isothermal value. When expansion is present, the second and third terms increases the predicted γ, since $n' < 0$ and $A', n'' > 0$. The contribution of the final term depends on the model for collision frequency.

Typically, a lack of collisions implies $\gamma = 1$; however, in the case of an expanding nozzle, small but finite collision frequency with a Fourier model for heat flux in fact implies a γ somewhat greater than unity. This has been shown theoretically by Little and Choueri [2], who found a low collision limit of $\gamma \approx 1.16$ for their magnetic field geometry.

To predict a value between the two limits, we require a form for ν. The standard form takes that of classical electron-electron or electron-ion collisions, $\nu_e \approx 4 \times 10^{-12} n \ln\Lambda / T_e^{3/2}$ [16], where $\ln\Lambda$ is the Coulomb logarithm and T_e is in eV. This form has been studied previously by Little and Choueri and indeed predicts a value of γ comparable to what is observed. However, this collision frequency is admittedly insufficient to inhibit electron heat flux in magnetic nozzles. Applying a Fourier law in this study results in a total heat flux downstream that is larger than the power being delivered to the thruster. However, the fact remains that the theory may be predictive if the collision frequency were higher.

One way for the effective collision frequency to be higher than the classical prediction is through nonlinear interactions between particles and waves. This enhancement to the typical collision frequency has been observed in many plasmas [12, 18, 19] and may induce an effective collision frequency orders of magnitude higher than the classical equivalent. Furthermore, we have recently published a study [7] that shows that a lower hybrid drift instability exists in the plume of a magnetic nozzle, and the effective collision frequency of this mode is several orders of magnitude higher than the classical value. This instability may further influence electron heat transfer in a magnetic nozzle via an enhancement to the electron Ohm's law. We elaborate on this concept in the following section.

E. Anomalous electron collision frequency from waves

To motivate how instabilities can drive anomalous resistance, we start from the Vlasov equation:

$$\frac{\partial f}{\partial t} + \mathbf{v}\cdot\frac{\partial f}{\partial \mathbf{x}} + \frac{q}{m}\left(\mathbf{E} + \mathbf{v}\times\mathbf{B}\right)\cdot\frac{\partial f}{\partial \mathbf{v}} = 0 \tag{19}$$

where f is the species distribution function, t is time, $\mathbf{v}$ is the velocity coordinate, $\mathbf{x}$ is the position coordinate, $\mathbf{E}$ is the electric field, and $\mathbf{B}$ is the magnetic field. The right hand side typically represents a collision operator, but we assume the plasma of a magnetic nozzle to be classically collisionless. To derive the impact of waves on the steady-state particle distribution, we may isolate the steady state values by performing a phase average.

We begin by perturbing the distribution $f = f_0 + f_1$ and the electric field, $\mathbf{E} = \mathbf{E}_0 + \mathbf{E}_1$, where the subscript 1 indicates a small, oscillatory quantity. In general, we may further perturb the magnetic field. However, the magnitude of this impact is related to the plasma β, and the β for low temperature plasmas such as ours is typically small. We may further specify the perturbation by assuming a sinusoidal character, $f_1, \mathbf{E}_1 \propto e^{i(-\omega t + \mathbf{k}\cdot\mathbf{x})}$, where ω is the frequency and $\mathbf{k}$ is the wavevector. To isolate the steady-state values, we will perform a phase average on the entire equation. Each quantity that is of first order in the perturbed quantities will vanish since the perturbations are periodic. The only term that remains is the second order term:

$$\frac{\partial f_0}{\partial t} + \mathbf{v}\cdot\frac{\partial f_0}{\partial \mathbf{x}} + \frac{q}{m}\left(\mathbf{E_0} + \mathbf{v}\times\mathbf{B}\right)\cdot\frac{\partial f_0}{\partial \mathbf{v}} = -\frac{q}{m}\langle \mathbf{E}_1\cdot\frac{\partial f_1}{\partial \mathbf{v}}\rangle \tag{20}$$

Downloaded by UNIV OF MICHIGAN on August 31, 2021 | http://arc.aiaa.org | DOI: 10.2514/6.2021-3399

where $\langle\cdot\rangle$ represents a phase average. This result shows that a wave may act as an effective collision operator on the steady-state distribution.

To determine the impact of waves on measurable, fluid quantities, we may take successive moments of Eqn. 20. First, taking the zeroth moment (integrating both sides over velocity space) yields the unchanged continuity equation:

$$\frac{\partial n_0}{\partial t} + \frac{\partial}{\partial \mathbf{x}} \cdot (n\mathbf{u}) = 0 \tag{21}$$

where the right hand side of Eqn. 20 disappears after integration by parts.

Taking the first moment of Eqn. 20 (i.e. multiplying the entire equation by $m\mathbf{v}$ then integrating over velocity space) gives the modified momentum equation:

$$nm\frac{\partial \mathbf{u}}{\partial t} + nm\mathbf{u}\cdot\frac{\partial \mathbf{u}}{\partial \mathbf{x}} = nq\left(\mathbf{E} + \mathbf{u}\times\mathbf{B}\right) - \frac{\partial P}{\partial \mathbf{x}} + q\langle n_1\mathbf{E}_1\rangle \tag{22}$$

$$= nq\left(\mathbf{E} + \mathbf{u}\times\mathbf{B}\right) - \frac{\partial P}{\partial \mathbf{x}} + \mathbf{R}_{an}. \tag{23}$$

Here, we have assumed that the anomalous force can be modelled as a resistivity between electrons and ions (to be proven in Sct. II.F) as $\mathbf{R}_{an} = mn\bar{\nu}_{an}(\mathbf{u}_e - \mathbf{u}_\mathbf{i})$, where $\bar{\nu}_{an}$ is the effective, or "anomalous" collision frequency tensor. We consider this to be a diagonal tensor and write it in this form only to imply that it is not necessarily isotropic. Explicitly, in the direction parallel to the magnetic field, we find

$$\nu_{an,\parallel} = \frac{q\langle n_1 E_{1,\parallel}\rangle}{mn(u_{e,\parallel} - u_{i,\parallel})}. \tag{24}$$

Physically, waves retard motion of electrons as they extract energy to grow, which acts as an effective collision frequency. This modified value may be used in lieu of classical collisions in the heat transport term [20], such that $\nu_e \longrightarrow \nu_{AN}$ in the Fourier law of Eqn. 14.

To evaluate this term, we need a full form for the anomalous resistivity $q\langle n_1 E_{1,\parallel}\rangle$ and the relative velocity $u_{e,\parallel} - u_{i,\parallel}$. We begin with the former and return to the relative velocity at the end of this section.

F. Expression for anomalous collision frequency in low temperature nozzle

The phase averaged terms are difficult to evaluate in their current forms. However, with knowledge of the nature of the waves in question, we may rewrite these in more tractable forms. To this end, we begin with Gauss' law for electric fields:

$$\nabla \cdot E = \frac{\rho}{\epsilon_0}. \tag{25}$$

Again assuming a periodic nature of the electric field, we may rewrite this as

$$i\mathbf{k}\cdot\mathbf{E}_1 = \frac{e}{\epsilon_0}\sum_s Z_s n_{1,s} \tag{26}$$

in which we have defined $\mathbf{k}$ as the wavevector and Z_s as the charge state of the species. Here we have also assumed a similar law for the steady state values, $\nabla\cdot\mathbf{E}_0 = \frac{e}{\epsilon_0}\sum_s Z_s n_{0,s}$.

Rearranging Eqn. 26 provides us with the dispersion relation:

$$0 = 1 + \sum_s \chi_s \tag{27}$$

where we have defined the susceptibility

$$\chi_s \equiv \frac{iZe}{\epsilon_0}\frac{n_{1,s}}{\mathbf{k}\cdot\mathbf{E}_1}. \tag{28}$$

The susceptibility is generally a complex value that represents the response of a species to an electric field, both in magnitude and phase offset. Using this value, we may rewrite the wave-induced resistivity as

$$q\langle n_1\mathbf{E}_1\rangle = \langle E_1^2\frac{\epsilon_0}{i}\mathbf{k}\chi_s\rangle \tag{29}$$

$$= \int \epsilon_0 E_1^2(\mathbf{k})\mathbf{k}\mathrm{Im}(\chi_s)d\mathbf{k} \tag{30}$$

Downloaded by UNIV OF MICHIGAN on August 31, 2021 | http://arc.aiaa.org | DOI: 10.2514/6.2021-3399

Downloaded by UNIV OF MICHIGAN on August 31, 2021 | http://arc.aiaa.org | DOI: 10.2514/6.2021-3399

where we have applied a Fourier transform of E_1 to evaluate the phase average. From Eqn. 30 and 27, we observe that, for a plasma with only electrons and singly ionized ions, $\mathrm{Im}(\chi_e) + \mathrm{Im}(\chi_i) = 0$ and $\mathbf{R}_{an,i} = -\mathbf{R}_{an,e}$. Thus we see that the presence of an oscillation serves as a means of transferring momentum between electrons and ions. This fact serves as motivation to define the force as an effective resistivity between electrons and ions as in Eqn. 24.

To determine the electron susceptibility, we may perform a different operation on Eqn. 19. Namely, perturbing the distribution function and electric field but neglecting higher order terms (as opposed to phase averaging) provides a direct relation between n_1 and E_1. For the plasma in question, we may make the following assumptions:

- Electrons are isothermal across the magnetic field.
- The magnetic field is uniform and steady.
- Classical collisions are negligible compared to electromagnetic forces on both species.
- Ions are cold and unmagnetized.

- The steady state electron number density is quasi-Maxwellian, with an asymmetric component induced by the cross-field number density gradient.

Finally, the electron steady state distribution function is assumed to be quasi-Maxwellian, incorporating an asymmetric factor in the azimuthal drift direction as

$$f_{e,0}(\mathbf{v} = \left(1 - \frac{1}{n_e}\frac{\partial n_e}{\partial \perp}\frac{m_e v_\theta}{eB}\right) F_{\mathrm{M},e}, \tag{31}$$

where $F_{M,e}$ is a Maxwellian distribution function.

The final dispersion relation is found upon integrating the perturbed Vlasov equation along unperturbed orbits using the method of characteristics. This process has been described in previous references [21] and leads to an electron susceptibility of

$$\chi_e = \frac{1}{k^2\lambda_D^2}\left[1 + \frac{\omega - k_\theta(v_D + v_E)}{k_z v_{te}} e^{-k_\theta^2 r_L^2/2} I_0\left(\frac{k_y^2 r_L^2}{2}\right) Z\left(\frac{\omega - k_\theta v_E}{k_\parallel v_{te}}\right)\right]. \tag{32}$$

Here, I_0 is a modified Bessel function of the first kind, Z is the plasma dispersion function, v_{te} is the electron thermal velocity, r_L is the electron Larmor radius, λ_D is the Debye length, and v_D and v_E is the electron diamagnetic and $E \times B$ drift velocities, respectively. We may then find the wave-induced resistivity by inserting this value into Eqn. 30. We further may relate k to ω using the full dispersion relation from Eqn. 27,

$$0 = 1 - \frac{\omega_{p,i}^2}{\omega^2} + \chi_e \tag{33}$$

where the second term represents the cold, motionless ion susceptibility, and $\omega_{p,i}$ is the ion plasma frequency. This wave derives its energy for growth from the electron diamagnetic drift. It then acts as a medium for transferring the electron momentum lost into the ions. This transfer acts as an effective resistivity to the electrons and induces a cross-field electron transport akin to a higher electron-ion collision frequency, as we have observed in a previous work [7]. However, our previous work also observed that the wave propagated parallel to the magnetic field with a comparable magnitude to its azimuthal component. This fact implies that the same energy and momentum transfer is likely happening between the waves, the electrons, and the ions in the parallel direction (as per Eqn. 24). While the lower hybrid drift instability theory does not incorporate finite electron or ion velocities parallel to the field, it is likely that they are still flowing relative to each other based on their differing rates of attachment to the magnetic fields [22]. This relative velocity may form the source of the resistivity in this direction and might encourage such a strong parallel propagation.

With a sufficient understanding of the wave that we observe, we are now ready to return to our evaluation of the relative drift velocity.

G. Relative velocity

To evaluate Eq. 24, we must estimate the relative magnitude $u_{e,\parallel} - u_{i,\parallel}$ via a few approximations. First, we take the electrons to follow their continuity equation, namely $(nuA)' = 0$. We solve this equation for the velocity and find

$$u_{e,z} = u_0 \exp\left(\int_3^z \frac{nA}{(nA)'} dz'\right) \tag{34}$$

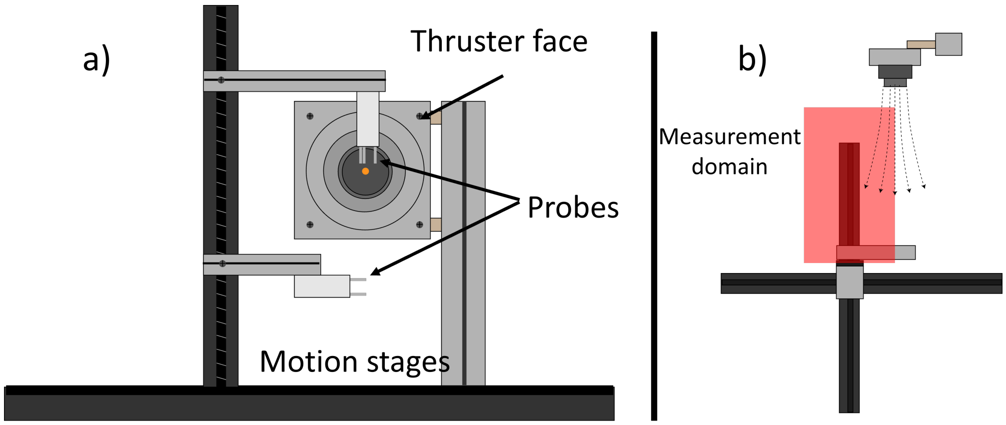

Fig. 2 Illustration of the experimental setup from the a) front-on and b) top-down perspective.

where u_0 is the condition assumed at our most upstream measurement point, $z = 3$ cm. The ions are unmagnetized and are thus less likely to expand with the field lines. Instead, they are likely to be accelerated only by the plasma potential gradient as

$$u_i = \sqrt{\frac{2q}{m_i}(\phi - \phi_0) + u_0^2}. \tag{35}$$

We estimate a final velocity of 10 km/s based off of previous ion velocity measurements [23] to return an initial u_0 of 7 km/s, which we use for both electrons and ions. While physically motivated, these values are still merely approximate. Given the uncertainty in these velocities, we elect to allow a parameter β in front of the velocity difference such that $u_{e,\parallel} - u_{i,\parallel} \to \beta(u_{e,\parallel} - u_{i,\parallel})$. We will assume $\beta = 1$ presently but will discuss its variation in Sct. V.

Now that we have established the theoretical framework required to evaluate Eqn. 24, we proceed to outline the experiment that we performed to test our hypothesis.

III. Experiment

We next briefly explain the experimental apparatus we used in this experiment to investigate this theory as presented in Fig. 2. As this is the same data set used in Ref. [7], we will only briefly repeat the process here. We performed the experiment on an electron cyclotron resonance thruster at the University of Michigan, which we operated at 17 W delivered power and a 2 sccm-Xe flow rate. We operated in the Junior vacuum facility, which is a 1m diameter and 3m length facility with a cryogenic pump. This setup allowed us to test at a backpressure of 4.3×10^{-6} Torr as measured on the wall.

We first measured the magnetic field using a Lakeshore Gaussmeter and three-dimensional Hall probe. We positioned the Hall probe on a set of orthogonal motion stages at atmosphere and took readings in 5 mm steps. We mapped the streamlines and found the outermost field line that intercepted the thruster to define the effective area A as a function of distance downstream.

To measure waves in the context of a magnetic nozzle, we implemented the technique of Beall [24] in situating a set of tungsten electrostatic probes downstream of the thruster. Each probe measured 5 mm in length and 1 mm in diameter. In biasing them to ion saturation levels, we can take relative fluctuations in the current readings as relative density fluctuations, $\tilde{n}/n$. Knowing the distance between the two and finding the phase difference of each frequency between the two probes provides the wavenumber and can be used to directly measure the dispersion. In using this technique, we are able to determine ω and $\mathbf{k}$.

We further used one of these probes in a second sweep across the plume as a Langmuir probe to determine background plasma properties. We applied the Druyvesteyn technique to analyze the electron energy distribution function [25] to find an effective number density and electron temperature, and considered the maximum of the first derivative of the electron current to be the plasma potential [26]. Figure 2 illustrates this setup. The measurement domain for all of these values was the axial region between $z = 3$ cm and $z = 14$ cm, with the radial measurements extending out to the outermost field line.

Downloaded by UNIV OF MICHIGAN on August 31, 2021 | http://arc.aiaa.org | DOI: 10.2514/6.2021-3399

Downloaded by UNIV OF MICHIGAN on August 31, 2021 | http://arc.aiaa.org | DOI: 10.2514/6.2021-3399

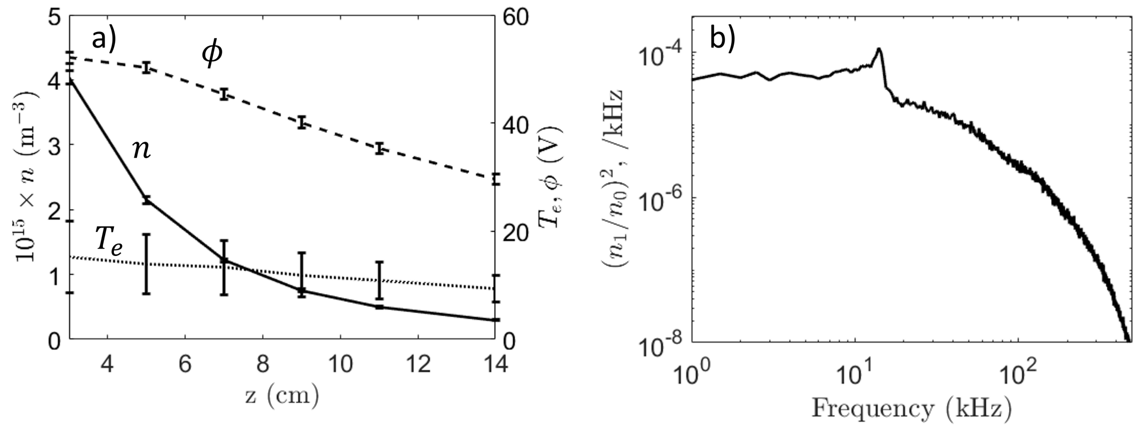

Fig. 3 a) Number density, plasma potential, and electron temperature as a function of axial position. b) Sample power spectral density taken from a point 7 cm downstream and 2.5 cm off-axis.

IV. Results

We present in Fig. 3a the one dimensional electron temperature, plasma potential, and number density as measured by the Langmuir probes. In these figures, we have averaged over the effective area as outlined in Fig. 1. We note a few expected trends in this dataset. First, the plasma potential drops monotonically downstream as the electron temperature decreases as well. The commonly understood relation between these two values is $\phi' = (nT_e)'/n$ resulting from the electron Ohm's law. Physically, this equality represents the exchange of energy between ions and electrons. As the electrons cool, the ions accelerate through the potential drop. These values indeed vary following this relation in the present work. The number density similarly decreases downstream as the effective area of the nozzle increases and the plasma expands. This too is expected from continuity, since as the plasma expands and accelerates the number density must decrease.

We can use the correlation between number density and electron temperature to calculate γ by $\gamma = 1 + \frac{\ln(\hat{T})}{\ln(\hat{n})}$. Figure 3b shows this result through the plume. We note that we have removed the first point at 3 cm downstream, which we used as the reference for the normalization and thus has an undefined γ. This result reveals an average γ of ≈ 1.15, which lies between the isothermal and adiabatic limits. This result is within the range of what has been observed in similar systems [2–4] and is thus expected.

Using the results from the Langmuir probe, we may calculate the classical electron-ion collision frequency [27]. While we have already discussed the general lack of classical collisions in these plasmas, it is nevertheless instructive to observe the magnitude and implications to compare them to the anomalous values. We report the classical collision frequency in Fig. 4b and the predicted heat flux in Fig. 5. We do not present the predicted value of γ in Fig. 4a, since this calculation predicts a fully isothermal plasma in this situation. This is a noteable departure from the previous work studying the relation between classical collisions and γ, which showed a lower limit of 1.16 [2]. The primary reason for this departure may lie in the lower value of A'/A in our nozzle. The previous work used a nozzle produced by current carrying coils, whereas the current one is generated by a series of permanent magnets that may not maintain the same expansion profile. Since the expansion causes the non-isothermal value in Ref. [2], decreasing the relative expansion rate will drive the electrons more isothermal.

We also reconfirm the physical discrepancy that arises in that heat conduction limited only by classical collisions is far too high– in our case, several orders of magnitude higher than the power we delivered to the thruster. Again, this result was also found in Ref. [2] and is thus expected. However, the discrepancy in the previous work was a single order of magnitude, whereas ours is at least three. The reason for this difference is the drastically reduced classical electron collision frequency in our plasma. The previous work reported number densities up to three orders of magnitude higher than what we find in the present work and electron temperatures lower by several eV. As the Coulombic collision frequency is proportional to $n/T_e^{3/2}$, these differences drastically alter the value between the two plasmas.

Now that we have measured γ directly and found the implications of classical theory, we can analyze the results from the wave observations. Figure 3b presents an example power spectral density of density oscillations at a point 7 cm downstream from the exit plane and 2.5 cm off-axis, where we have averaged the results from the two probes

Downloaded by UNIV OF MICHIGAN on August 31, 2021 | http://arc.aiaa.org | DOI: 10.2514/6.2021-3399

oriented in the azimtuhal direction. We characteristically observe a decay of wave magnitude as the frequency increases and can identify this incoherent mode with a lower hybrid drift instability [7]. We further note a coherent mode at a lower frequency, but we believe that this is likely a separate mode so we have removed it from the present analysis. We use the value $(n_1/n_0)^2$ in Eqn. 30 after substituting for it in terms of E_1 and χ_e as per Eqns. 28 and 32. Numerically, we separate the power spectral density into bins of 500 Hz then take the integral to be

$$q\langle n_1 E_{1,\parallel}\rangle \approx \sum_{k_\theta} \epsilon_0 E_{1,z}^2 k_\parallel \mathrm{Im}(\chi_e)\Delta k_\theta \tag{36}$$

where Δk_θ is the 500 Hz bin width and the electric field oscillation magnitude $E_{1,z}$ represents the power spectral density of oscillations over the bin width.

Since the summation in Eqn. 36 is over k_θ but incorporates $k_\parallel$, we further require a relation between the two. Experimentally, we find that the parallel propagation is linear and comparable to the azimuthal propagation (see Fig. 3 of Ref. [7]). Since we have measured the waves in r and z, we cannot directly deduce the wavenumber parallel to the field line. However, we may project the (r, z) propagation onto the field line by analyzing the phase velocity. The phase velocity is given by $v_\phi = \omega/k$ and takes a different value in each direction. We may use these measurements to find $k_\parallel/k_\theta$ with

$$\frac{k_\parallel}{k_\theta} = \frac{k_r B_r + k_z B_z}{B k_\theta} \tag{37}$$

$$= \frac{B_z/v_{\phi,z} + B_r/v_{\phi,r}}{B/v_{\phi,\theta}}. \tag{38}$$

We present the average magnitude of this value in Fig. 5b, observing that the parallel propagation is stronger upstream but is dominated by the azimuthal propagation downstream.

We may use the magnitude of the oscillation n_1/n_0 as a function of frequency with Eqn. 28 and 32 to calculate $E_{1,z}$. We may then use this result in Eqn. 30 to find the anomalous resistivity, which we finally insert into Eqn. 24 to find the anomalous collision frequency in the field-aligned direction. We present this value (averaged over each nozzle area downstream as per the quasi-1D geometry) in Fig. 4. We compare it on the same axes to the value predicted via classical electron-ion collisions which we see to be orders of magnitude less than the anomalous equivalent.

We have already reported the anomalous collision frequency in the azimuthal direction in Ref. [7] and do not replicate those results in this work. We present here instead the parallel collision frequency $\nu_\parallel$ in Fig. 4b and the classical equivalent ν_c. It is clear from this data that throughout the plume the anomalous collision frequency is at least three orders of magnitude higher than the classical value, motivating the idea that it may contribute to supporting the temperature gradients and predict the observed polytropic index.

Finally, we may apply these results to find the total heat flux q via the Fourier law (Eqn. 14) and the predicted polytropic index from the anomalous collision frequency using Eqn. 24 and 17. After finding the heat flux, we solve Eqn. 17 numerically. Since it is often multi-valued, we choose the result that lies between 1 and 5/3, as these are the physical limits that γ should take. Fig. 4a presents the resulting polytropic index, and Fig. 5a indicates the total down stream heat flux as a function of position for both the classical and anomalous case. The total power delivered to the thruster is also labelled at 17 W. We observe that the anomalous heat flux is comparable to the delivered power (albeit slightly higher in the upstream regions), whereas the value predicted from classical collisions is 4 orders of magnitude higher. The trend that we observe in this value is expected. Initially, the heat flux is high from the large values of n and T_e. These values decay downstream as the energy stored in the pressure is converted to ion kinetic energy. The heat flux again begins to rise as the anomalous collision frequency trends downwards, but this may be accounted for by analyzing the various error sources we discuss in the following section.

V. Discussion

These results reveal that a description of the electron heat flux implementing a Fourier law with an anomalous electron collision frequency predicts a polytropic index comparable to what is observed, i.e 1.15. Moreover, inclusion of the anomalous collision frequency reduces the predicted heat flux downstream by several orders of magnitude compared to the classical value. Moreover, the maximum predicted heat flux approaches the power delivered to the thruster. This is a notable difference from previous work discussing heat flux in a magnetic nozzle with a Fourier law [2], who found that the heat flux was too high. Indeed, it appears that the inclusion of anomalous effects may constrain the heat flux

Downloaded by UNIV OF MICHIGAN on August 31, 2021 | http://arc.aiaa.org | DOI: 10.2514/6.2021-3399

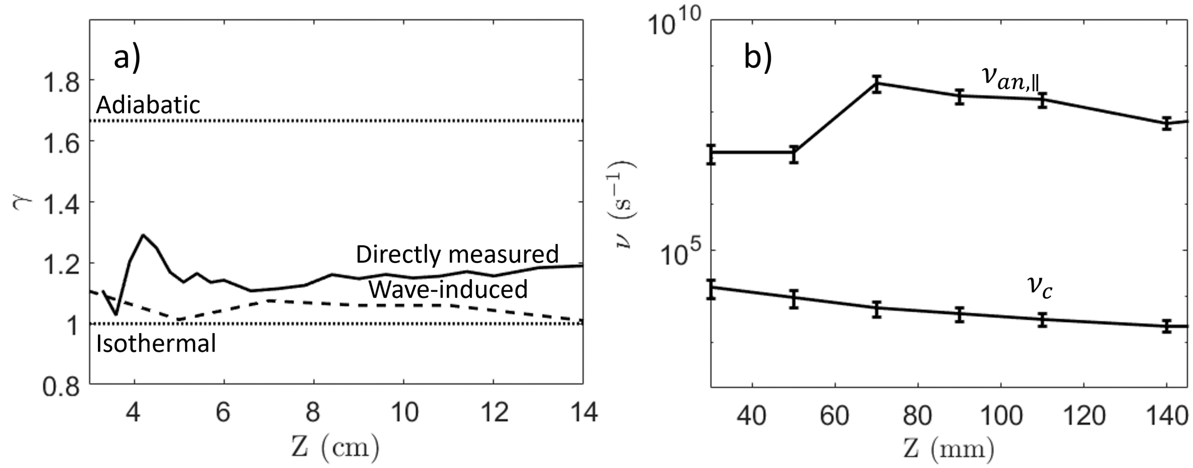

Fig. 4 a) γ predicted from waves and directly measured. Error bars are roughly 15% but have been left off for clarity. b) Effective collision frequency in the field-aligned direction ($\nu_{an,z}$) and classical collision frequency (ν_c).

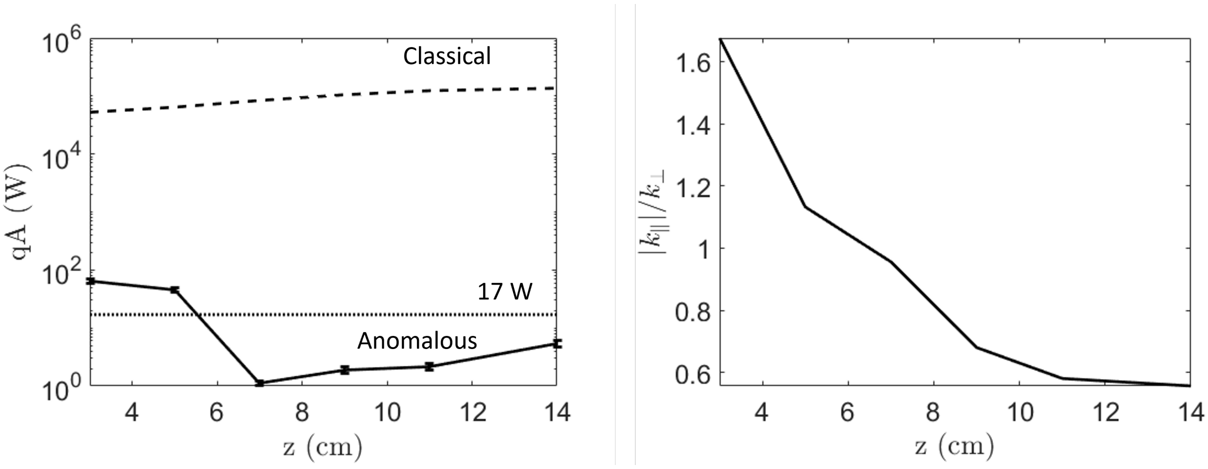

Fig. 5 a) Total heat flux through the nozzle predicted by classical collisions and anomalous effects. Error bars are on the order of 10%, which do not appear on a logarithmic scale and are thus omitted.

to more physical levels. This is reminiscent of our previous work as well, which indicates that these effects likely contribute to electron momentum across field lines [7]. Thus, while classical collisions are likely insufficient to affect the expansion in a typical nozzle, instabilities may play a significant role.

The trend in heat flux is also generally representative of what we expect for this device. As the plasma expands downstream, we expect the heat flux to decay as the thermal energy is converted into ion bulk energy. We indeed observe a sharp decrease in anomalous heat flux between 5 and 7 cm downstream, which may reflect this energy transition.

However, two inconsistencies emerge with our results. First, the total heat flux upstream of 5 cm remains higher than the total delivered power by roughly a factor of 4. While this is significantly closer than the classical prediction, it is still unphysical. Second, the heat flux appears to rise downstream of 7 cm. The precise reason for this trend is not clear. However, there are several potential modifications to the theory that may be able to explain these phenomena.

The inconsistencies in our measurements may stem in part from the assumptions underlying our model. For example, we make a strong assumption by using a Fourier law and simply replacing the collision frequency with an anomalous one. The derivation of the Fourier law for heat conduction in the classical case starts with the Boltzmann equation with a classical collision operator incorporating electron collisions with ions as well as with other electrons. In effect, by employing an expansion approximation, it is shown that the balance of collisions can lead to asymmetries on the

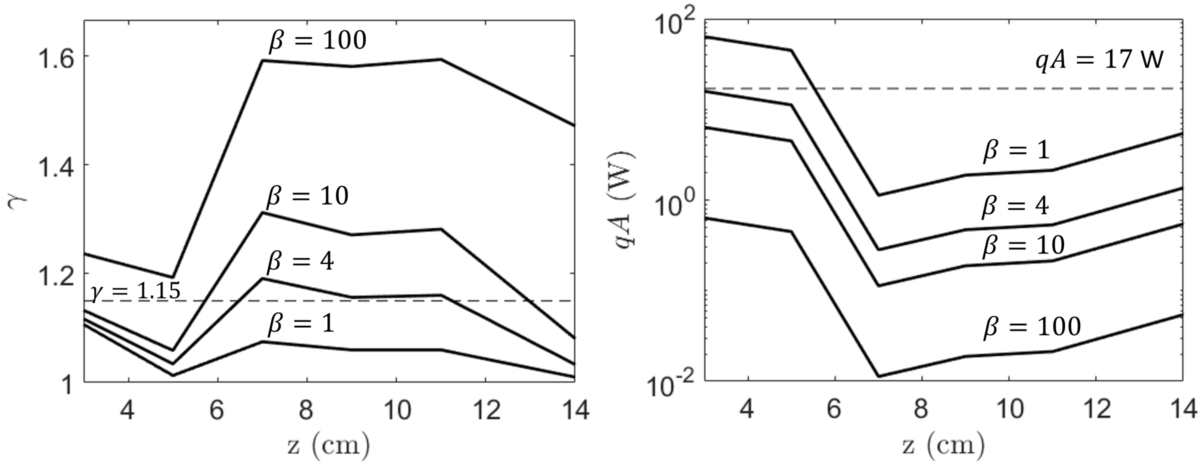

Fig. 6 a) Polytropic index with varying collision frequency scaling factors with the observed 1.15 illustrated by the dashed line. b) Predicted heat flux downstream as a function of space for varying collision frequency scaling with the thruster power illustrated by the dashed line.

velocity distribution that in turn result in finite heat flux. The scaling of this heat flux follows an Onsager relationship, i.e. a Fourier law moderated by the classical electron collision frequency. It is not clear from a first principles analysis that a kinetic collision operator based on the wave-particle interaction will yield a similar form. We have made this assumption out of expedience. However, for a full description of the interaction between waves and heat flux, a new formalism should be developed starting with the kinetic wave collision operator [20].

The second simplifying assumption we have made is about the magnitude of the relative drift between electrons and ions. This was necessitated ultimately by the challenge in directly inferring the electron velocity. It is difficult to accurately derive a magnitude for $\nu_{an,z}$ as per Eqn. 24. To briefly explain why, we begin by understanding that a magnetic nozzle is globally current-free, given that there are no electrodes exchanging current with the plasma. Thus, integrating the net current density over the plasma volume must equal zero. While we approximate this value as illustrated in Eqn. 34 and 35, observation of Eqn. 24 implies that the collision frequency is quite sensitive to this approximation. To investigate this sensitivity, we may return to the parameter β defined in Sct. II that acts as a control for the relative velocity.

To explore the variation of the results on γ and q, we may look at the results when changing β freely. In increasing β, we are thus increasing the relative velocity and decreasing the overall heat flux. To this end, we present the resulting γ and heat flux for $\beta = 1, 4, 10$, and 100 in Fig. 6. These results show that by multiplying the collision frequency by a factor of 4, the predicted γ matches the experiment more closely and the total heat flux downstream is universally less than the power delivered to the thruster. As this value increases further, γ begins to approach the adiabatic limit as expected, and the previously lower values approach the observed value. While we have multiplied the relative velocity by a universal factor, it is also likely that our approximation breaks down to a different extent for each point. Thus, perhaps at 5 cm a value of β closer to 50 is necessary, whereas a value of 4 works for 9 cm downstream, implying that the electrons and ions are moving with a larger relative velocity downstrem. Moreover, the heat flux terms may exhibit similar trends. While a universal factor of 4 decreases the predicted heat flux below the total value, given that electron convection and ion kinetic energy must also draw from the thruster input, it is unlikely that the full power is going to electron heat flux, and this β value is likely higher upstream. The fact that this trend appears in both the γ and total heat flux calculation lends credence to such a variation.

As a final comment on a possible modification to our approach, there remains the possibility that Ohmic heating and thermal energy transfer between particle species and waves may be significant. Whereas we have neglected these values in Eqn. 3, two new terms appear on the right hand side when the direct wave effects are included:

$$\frac{3}{2}\frac{\mathrm{d}nT}{\mathrm{d}t} + \frac{5}{2}nT\nabla\cdot\mathbf{u}_\sigma = -\nabla\cdot\mathbf{q} + q\left(n_0\langle\mathbf{E}_1\mathbf{v}_1\rangle - \mathbf{v}_0\cdot\langle\mathbf{E}_1 n_1\rangle\right) \tag{39}$$

where we have defined $\mathbf{v_1} = \int \mathbf{v} f_1 d\mathbf{v}$. The second term on the right hand side represents an effective collisional thermal

Downloaded by UNIV OF MICHIGAN on August 31, 2021 | http://arc.aiaa.org | DOI: 10.2514/6.2021-3399

energy transfer between the electrons and the waves, and the final term represents Ohmic heating from the anomalous resistivity. These two terms may represent significant heating contributions and modify our results.

VI. Conclusion

In this work, we have presented a theory for determining anomalous heat conduction along magnetic field lines in a magnetic nozzle. We have defined an anomalous collision frequency that represents momentum exchange between electrons and ions. This method implements quasilinear resistivity and assumes that the anomalous collision frequency in the momentum equation may also be used in an electron Fourier law. This is a reasonable assumption, since electron heat conduction may indeed be impeded by the momentum exchange interaction between species. However, a full treatment would require an effective electron-electron collision frequency as well as the incorporation of Ohmic heating and heat transfer derived from the Boltzmann equation.

We then applied our theory to experimental data on an electron cyclotron resonance thruster. We directly measured the plasma properties and found a polytropic index of 1.15. We compared this to wave measurements, which we used in our theory to predict heat flux and a non-adiabatic polytropic index. We find a agreement to within 15% over the domain; however, as we have presented the theory the total heat flux downstream is greater than the power delivered to the thruster within 6 cm of the thruster exit, and the predicted γ is too low. It is found that decreasing the assumed relative velocity between ions and electrons by a factor of 4 corrects these values and matches match the data. This work ultimately represents a critical step in a more thorough understanding of the wave-particle interactions that affect magnetic nozzle thermodynamics. This insight may in turn be leveraged to arrive at self-consistent descriptions for thruster operation and performance.

VII. Acknowledgments

This work was funded under NASA Space Technology and Research Fellowship Grant No. 80NSSC17K0156. We would like to thank the members of the Plasmadynamics and Electric Propulsion Lab for the insightful conversations.

References

[1] Merino, M., and Ahedo, E., “Influence of electron and ion thermodynamics on the magnetic nozzle plasma expansion,” *IEEE Transactions on Plasma Science*, Vol. 43, No. 1, 2015, pp. 244–251. https://doi.org/10.1109/TPS.2014.2316020, URL http://www.ieee.org/publications_standards/publications/rights/index.html.

[2] Little, J., and Choueiri, E., “Electron Cooling in a Magnetically Expanding Plasma,” *Phys. Rev. Lett.*, Vol. 117, No. 225003, 2016. URL https://journals.aps.org/prl/pdf/10.1103/PhysRevLett.117.225003.

[3] Collard, T. A., and Jorns, B. A., “Magnetic nozzle efficiency in a low power inductive plasma source,” *Plasma Sources Sci. Technol.*, Vol. 28, No. 105019, 2019. https://doi.org/10.1088/1361-6595/ab2d7d.

[4] Takahashi, K., Charles, C., Boswell, R. W., and Ando, A., “Thermodynamic Analogy for Electrons Interacting with a Magnetic Nozzle,” *Physical Review Letters*, Vol. 125, No. 16, 2020, p. 165001. https://doi.org/10.1103/PhysRevLett.125.165001, URL https://link.aps.org/doi/10.1103/PhysRevLett.125.165001.

[5] Zhang, Y., Charles, C., and Boswell, R., “Measurement of bi-directional ion acceleration along a convergent-divergent magnetic nozzle,” *Appl. Phys. Lett.*, Vol. 108, No. 10, 2016, p. 104101. https://doi.org/10.1063/1.4943583, URL http://aip.scitation.org/doi/10.1063/1.4943583.

[6] Ahedo, E., Correyero, S., Navarro, J., and Merino, M., “Macroscopic and parametric study of a kinetic plasma expansion in a paraxial magnetic nozzle,” *Plasma Sources Science and Technology*, Vol. 29, No. 4, 2020, p. 045017. https://doi.org/10.1088/1361-6595/ab7855, URL https://doi.org/10.1088/1361-6595/ab7855.

[7] Hepner, S., Wachs, B., and Jorns, B., “Wave-driven non-classical electron transport in a low temperature magnetically expanding plasma,” *Appl. Phys. Lett*, Vol. 116, No. 263502, 2020. https://doi.org/10.1063/5.0012668.

[8] Hurtig, T., Brenning, N., and Raadu, M. A., “The Penetration Of Plasma Clouds Across Magnetic Boundaries: The Role of High Frequency Oscillations,” *Phys. Plasmas*, Vol. 11, No. L33, 2004. URL https://doi.org/10.1063/1.1753575.

[9] Hoh, F. C., “Instability of Penning-Type Discharges,” *Physics of Fluids*, Vol. 6, No. 8, 1963, pp. 1184–1191. https://doi.org/10.1063/1.1706878, URL http://aip.scitation.org/toc/pfl/6/8.

Downloaded by UNIV OF MICHIGAN on August 31, 2021 | http://arc.aiaa.org | DOI: 10.2514/6.2021-3399

[10] Krall, N. A., and Liewer, P. C., "Low-Frequency Instabilities in Magnetic Pulses," *Phys. Rev. Lett.*, Vol. 4, No. 5, 1971. URL https://journals.aps.org/pra/pdf/10.1103/PhysRevA.4.2094.

[11] Cavalier, J., Lemoine, N., Bonhomme, G., Tsikata, S., Honoré, C., Grésillon, D., Honor, C., and Gr Esillon, D., "Hall thruster plasma fluctuations identified as the electron drift instability: Modeling and fitting on experimental data," *Phys. Plasmas*, Vol. 20, No. 082107, 2013. https://doi.org/10.1063/1.4817743.

[12] Ducrocq, A., Adam, J. C., Héron, A., and Laval, G., "High-frequency electron drift instability in the cross-field configuration of Hall thrusters," *Phys. Plasmas*, Vol. 13, No. 102111, 2006. https://doi.org/10.1063/1.2359718.

[13] Janhunen, S., Smolyakov, A., Chapurin, O., Sydorenko, D., Kaganovich, I., and Raitses, Y., "Nonlinear structures and anomalous transport in partially magnetized E × B plasmas," *Phys. Plasmas*, Vol. 25, No. 1, 2018. https://doi.org/10.1063/1.5001206.

[14] Light, M., Chen, F. F., and Colestock, P. L., "Low frequency electrostatic instability in a helicon plasma," *Phys. Plasmas*, Vol. 8, No. 10, 2001. https://doi.org/10.1063/1.1403415.

[15] Litvinov, I. I., "Stationary efflux into a vacuum by a dual-temperature fully ionized plasma," *Journal of Applied Mechanics and Technical Physics*, Vol. 12, No. 6, 1971, pp. 793–802. URL https://link.springer.com/content/pdf/10.1007%2FBF00850447.pdf.

[16] Bellan, P. M., *Fundamentals of Plasma Physics*, Cambridge University Press, 2008.

[17] Braginskii, S. I., "Transport processes in a plasma," *Reviews of plasma physics, 1*, 1965.

[18] Brown, Z. A., and Jorns, B. A., "Spatial evolution of small wavelength fluctuations in a Hall Thruster," *Physics of Plasmas*, Vol. 26, No. 11, 2019, p. 113504. https://doi.org/10.1063/1.5116708, URL http://aip.scitation.org/doi/10.1063/1.5116708.

[19] Jorns, B., Lopez Ortega, A., and Mikellides, I. G., "First-principles Modeling of the IAT-driven Anomalous Resistivity in Hollow Cathode Discharges I: Theory," *52nd AIAA/SAE/ASEE Joint Propulsion Conference*, AIAA 2016-4626, Salt Lake City, UT, 2016. https://doi.org/10.2514/6.2016-4626, URL http://arc.aiaa.org/doi/10.2514/6.2016-4626.

[20] Dum, C. T., "Anomalous electron transport equations for ion sound and related turbulent spectra," *The Physics of Fluids*, Vol. 21, No. 6, 1978, p. 956. https://doi.org/10.1063/1.862339, URL https://aip.scitation.org/doi/abs/10.1063/1.862339.

[21] Carter, T. A., Ji, H., Trintchouk, F., Yamada, M., and Kulsrud, R. M., "Measurement of Lower-Hybrid Drift Turbulence in a Reconnecting Current Sheet," *Phys. Rev. Lett.*, Vol. 88, No. 1, 2002. https://doi.org/10.1103/PhysRevLett.88.015001.

[22] Merino, M., and Ahedo, E., "Fully magnetized plasma flow in a magnetic nozzle," *Phys. Plasmas*, Vol. 23, 2016, p. 42. https://doi.org/10.1063/1.4941975, URL http://dx.doi.org/10.1063/1.4941975http://scitation.aip.org/content/aip/journal/pop/23/2?ver=pdfcov.

[23] Wachs, B., and Jorns, B., "Background pressure effects on ion dynamics in a low-power magnetic nozzle thruster," *Plasma Sources Sci. Technol.*, Vol. 29, No. 045002, 2020, p. 45002. https://doi.org/10.1088/1361-6595/ab74b6, URL https://doi.org/10.1088/1361-6595/ab74b6.

[24] Beall, J. M., Kim, Y. C., and Powers, E. J., "Estimation of wavenumber and frequency spectra using fixed probe pairs," *J. Appl. Phys.*, Vol. 53, No. 6, 1982. https://doi.org/10.1063/1.331279.

[25] Druyvesteyn, M. J., and Penning, F. M., "The mechanism of electrical discharges in gases of low pressure," *Reviews of Modern Physics*, Vol. 12, No. 2, 1940. URL https://journals.aps.org/rmp/pdf/10.1103/RevModPhys.12.87.

[26] Lobbia, R. B., and Beal, B. E., "Recommended Practice for Use of Langmuir Probes in Electric Propulsion Testing," *J Propul Power*, Vol. 33, No. 3, 2017, pp. 566–581. https://doi.org/10.2514/1.B35531, URL https://arc.aiaa.org/doi/10.2514/1.B35531.

[27] Spitzer, L., and Haem, R., "Transport phenomena in a completely ionized gas," *Phys. Rev.*, Vol. 89, No. 5, 1953, pp. 977–981. URL https://journals.aps.org/pr/pdf/10.1103/PhysRev.89.977.

Downloaded by UNIV OF MICHIGAN on August 31, 2021 | http://arc.aiaa.org | DOI: 10.2514/6.2021-3399